UCSD-SP 67-10

NsG-318

PRELIMINARY RESULTS OF THE UNIVERSITY OF CALIFORNIA X-RAY EXPERIMENT ON THE OSO-III

Laurence E. Peterson, Hugh S. Hudson

and Daniel A. Schwartz

University of California, San Diego

La Jolla, California

November 1967

Preliminary Results of the University of California X-Ray Experiment on the OSO-III*

Laurence E. Peterson, Hugh S. Hudson
and Daniel A. Schwartz
University of California, San Diego
La Jolla, California

I. Introduction

In this report we wish to describe the University of California X-ray experiment on the Third Orbiting Solar Observatory (OSO-111), indicate its present operational status and present a preliminary discussion of the results which have been obtained thus far. An OSO satellite consists of two parts: a telescope mount pointed at the sun and a rotating wheel member. The pointed section, which is maintained to within about 1 arc minute, contains instruments which generally cover the ultraviolet and soft X-ray range. The rotating wheel provides a stabilized platform for the pointed member, contains telemetry and servo systems and may be outfitted with additional experiments, generally of a somewhat different nature than those provided in the pointed section. The OSO's are launched into a nominally circular orbit of 33° inclination

*Based on presentations at the 13th International Astronomical Union Meeting, Prague, Czechoslovakia, August 21-30, 1967, and at the OSO-III Review Conference, Goddard Space Flight Center, October 6, 1967.

at 600 kilometers altitude, and are provided with tape recorder storage so that essentially complete data retrieval is obtained.

The University of California X-ray experiment in the OSO-III was located pointing radially outward in the wheel section and was designed to search for X-raysover the 7.7 to 210 kev region. The instrument scanned across the sun with every wheel rotation and, therefore, had the capability of observing hard solar X-ray emission. X-ray bursts have been observed previously from balloons and satellites and are generally associated with solar flares. Because of the extreme sensitivity of this instrument and its ability to maintain continuous operation during a period of increasing solar cycle activity, much more new information is being obtained on these X-rays, and the associated processes in the Atmosphere of the sun.

Cosmic X-rays were first discovered from rocket observations in 1962. Since that time instruments carried above the atmosphere by rockets and balloons have discovered numerous discrete sources of cosmic X-rays, and in addition have disclosed the presence of an apparently isotropic X-ray sky brightness. The OSO-III X-ray telescope is the first satellite-borne cosmic X-ray instrument. The X-ray sky map which it is generating is the first such survey in the energy range 7.7-210 kev. Valuable data on the variability of the cosmic X-ray sources are also the first of their kind.

The OSO-III was launched March 8, 1967. As of the present time, all satellite and experiment functions have been operating beyond expectations and the lifetime of the satellite is expected to be several

years, unless a catastrophic component failure occurs. This report presents results which have been obtained on cosmic and solar X-rays from preliminary processing and analysis of the data.

II. Experiment Description

The University of California instrument has been described in considerable detail previously! The detector, shown in Figure 1, consists of a 5 mm thick scintillation counter of about 10 cm^2 area surrounded by an anti-coincidence shielding collimator. The detector response, FWHM, is 24°; its solid angle is .15 steradians. The detector is arranged to look radially outward from the OSO wheel and as such scans across the sun, the sky, and the earth below with every nominally 2 second wheel rotation. As the spin axis of the wheel precesses in right ascension due to the servo controlled motion of the OSO, the wheel scan plane will eventually cover the entire celestial sphere.

Pulse-height information from the central detector is analyzed in six logarithmically spaced differential channels with a channel ratio of 1.7, and two integral channels at 7.7 kev and 210 kev. The first channel covers the range 7.7 to 12.5 kev, the second channel 12.5 to 22 kev, etc. Accumulation registers and logic are designed such that events from the sun and from the sky are processed in different manners. Information from each approximately .25 second scan across the sun is accumulated channel by channel in registers. Approximately 15 seconds are required to read out a complete 8 channel spectrum of the sun. Events which occur during the wheel scan are used to interrogate a direction scaler. This is referenced

to the sun during the day or to the spacecraft magnetometer during satellite night. The direction signature results in each 360^{o} sky-scan being broken up into approximately 60 six-degree wide intervals. Knowing the reference direction, the signature scaler number, the location of the satellite in geocentric coordinates and the position of the spin-axis in declination and right ascension, the arrival direction of each X-ray may be then obtained. Additional information such as the shield rates, and other quantities required to interpret the experiment are coded onto a subcommutator.

III. Status of Data Reduction

As of October 1, approximately 3 months of reduced data tapes have been received from the Goddard Space Flight Center. Of these tapes, approximately 1 month has been sent through the decommutation and reduction computer processing at UCSD. Most of this data is associated with the first few weeks of satellite operation. Certain additional intervals during which the sun was either exceptionally quiet or active have also been reduced. Orbital elements obtained fromthe predicted world maps sent are incorporated into a simple orbit computation program during the initial reduction. An aspect solution, required to determine the spin-axis of the satellite, is computed from the magnetometer data. The aspect is also checked with results obtained from GSFC and from a reduction obtained by the group at MIT for their cosmic y-ray experiment on the OSO-III. At the present time the aspect solution is undergoing review, although for the purposes of this paper there can be no doubt about the location of the spin axis. Final reduction will be accomplished

using the refined satellite orbital elements after the aspect solution is verified.

In addition to the main data reduction, we receive each day approximately five quick-look all channel printouts and associated punched tapes df X-ray experiment data from GSFC. These passes are obtained from the Ft. Meyers, Florida, tracking station. One orbit each day is reduced in a quick-look program to obtain updated information on the status of the experiment.

All the results reported here have been obtained from the final tapes received from the GSFC. The results quite naturally fall into two distinct groups; those obtained on cosmic X-rays and those obtained on solar X-rays.

IV. Cosmic X-Rays

The analysis required for cosmic X-rays is, of course, quite complex since the instrument is simultaneously scanning across the sky and moving in geomagnetic latitude and horizon aspect. The final programs for analyzing the cosmic X-ray results have not yet been completed and checked out. Certain results, however, are available at the present time. Figure 2 shows the regions of the celestial sphere which have been scanned as of October 1. The scan iine of the satellite wheel, as determined from our aspect solution, is shown on March 8 and October 1. Also shown is the scan line on May 11 indicating the effect of the finite detector aperture. The limits shown are the positions where the detector response is down one-half of its full response. The map of the celestial sphere also shows the location of some important cosmic X-ray sources which are known at the present time.

The results obtained from the scar of the sky during approximately ten orbits on May 11 are shown in Figure 3. May 11 was selected because at that time the sun was particularly quiet; even in the lowest channel there was no appreciable counting rate from the quiet sun. There were, however, two small X-ray bursts which, in fact, are visible in the data. Figure 3 shows the distribution of counts during the scan across the sky for both day and night intervals in the lowest channel, 7.7 to 12.5 keV. Data has been selected such that only events observed at times when the instrument was well above the earth's horizon are used. Direct effects due to earth albedo have, therefore, been eliminated. The background level produced by cosmic ray secondaries is averaged over all latitudes covered by the satellite. The gap during the night time is caused by part of the celestial sphere being occulted by the earth.

The relative intensities are obtained by dividing the number of counts observed in each sector interval by the normalized time that the detector was actually observing that sector interval. The details of this computation procedure will not be described here. However, for the data shown in Figure 3, each interval represents about one minute of data. The scan, as may be seen from Figure 2, crosses the sun, the galactic center and up into the northern skies. Sector numbers are referenced from the experiment solar eye turn-on which occurs 21^{o} before the instrument passes directly across the sun. The results in Figure 3 clearly show the sun, as indicated by the two small X-ray flares noted previously. The scan also shows the complex of X-ray sources near the galactic center and Scorpius XR-1. This latter strong source is shown in reduced intensity because, as may be seen from Figure 2, it lies outside the main aperture of the detector.

By obtaining scans such as these for the different energy channels and correcting for the background, one may obtain spectra of the various sources. By carefully fitting detector angular response functions to the scan distribution, one may obtain positions of strong sources to within a few degrees. The background when no strong sources are in the aperture is due mainly to the diffuse component of cosmic X-rays.

The preliminary results obtained on the cosmic background component will be discussed next. Studying such a component requires a detailed knowledge of the inherent background of the detector itself since this cannot be obtained by taking differences as the source moves across the aperture. The properties of the detector have been obtained in a series of balloon flights;[2] we know the true background of the detector and can correct accordingly. The method of extrapolation from the balloon results obtained over Palestine, Texas, to higher altitudes and lower latitudes has been worked out using data obtained from the University of Minnesota γ-ray experiment on the OSO-I.

The results obtained from the OSO-III are shown in Figure 4. The data averaged over the entire sky when the detector was above the horizon and when no strong sources were in the aperture are shown by the solid points. No correction has been made for satellite latitude except to eliminate intervals in the trapped radiation regions. Each point as a function of energy is corrected for the area, the detector aperture and the energy width of each channel to give a differential photon spectrum. To obtain the true cosmic component, one must correct for the detector background. This is neglectable at the lowest energies.

At the higher energies the detector background, obtained as discussed previously and shown in Figure 4 as a solid line, must be subtracted. This results in a steeply falling spectrum, shown by the dotted points.

Also shown as a solid line is the extrapolated spectrum obtained by the γ-ray spectrometer on the Ranger III.[3] The Ranger results, at least over the lower energy range, have since been verified in many rocket and balloon experiments.[4,5] The points obtained by the OSO-III are in excellent agreement with these data and, therefore, verify that the instrument is performing as expected. By a more careful analysis, using more data and correcting for latitude dependent background, considerably more precise information about the spectrum and particularly the anisotropy of the diffuse component of cosmic X-rays will be obtained on the OSO-III.

V. Solar X-Rays

As indicated previously, approximately two weeks of solar data have been examined in detail as well as certain other periods. Analyzing results from the sun is not particularly complex because of the data processor on board the satellite and the independence of results from orbital and aspect positions. The preliminary data analysis has generally confirmed the previous knowledge of solar X-ray emission.[6]

The outstanding characteristic of the sun in the hard X-ray region is its variability. The sun itself must be observed against the bright sky background due to the diffuse component of cosmic X-rays, discussed in the preceding section. During the period near May 11, the sun was invisible against this background because of the rather large solid angle aperture of the instrument. During the class 3 flare on March 22,

the counting rate completely saturated the electronics. The dynamic range of our instrument, measured by these extremes, is at least 50,000 to 1.

This experiment only observes effects in a small part of the solar electromagnetic spectrum covered by the instrument complement on the OSO-III satellite. The Air Force Cambridge Research Laboratory, under the direction of Dr. Hinteregger, has a spectrometer in the ultraviolet range. Dr. Neupert of the Goddard Space Flight Center[7] is operating a series of scanning crystal spectrometers which cover the range of approximately 400-1.3 Å. Both these instruments are mounted in the pointed section of the OSO. In the wheel section, in the same compartment as the UCSD experiment, Dr. Richard Teske of the University of Michigan[8] provided an X-ray ion chamber which covers principally the range between 8 and 12 Å.

Our experiment slightly overlaps the GSFC's spectrometer and observes the much harder component of X-rays. The 7.7-12.5 keV channel contains the shortest wavelength observed solar line at 1.6 Å. The dominant source of the counting rate in our lowest channels is not this line but rather a continuum emission, apparently due to thermal or non-thermal bremsstrahlung. This seems to maintain for either the quiet sun or for solar flare produced X-rays.

In Figure 5 are shown results on the "quiet" sun compared with those which have been obtained by rocket observations by the Lawrence Radiation Laboratory[9,10] during various portions of the present solar cycle. Here the coordinates have been chosen such that an exponential spectrum, characteristic of thermal bremsstrahlung, will appear as a straight line.

During June of 1965, the sun in this wavelength region could be characterized by a hot gas at 4.5 million degrees Kelvin. In the Fall of 1966 there was an emission component characteristic of a 15 million degree temperature. Our results are also shown on this same graph for two periods. One was during the first two weeks of satellite operation when the data has been extensively analyzed and the sun was generally active. Here the lowest flux was measured on March 15, 1967, when the two lowest channels gave a 36 million degree equivalent temperature. As indicated apreviously, during the period around May 11, 1967, the sun was invisible against the bright sky. Upper limits are shown for the lowest channel.

Some of these results, as well as those which follow, are summarized in Table I, which indicates for various conditions the counting rate, the energy flux in the lowest channel, and certain other parameters. Although it is unlikely that all the emission is caused by strictly thermal processes, it is possible under this assumption to obtain a temperature based on the data. From the measured flux, one may then obtain $\int N_e^2 \, dV$. For the quiet sun on March 15, when the equivalent temperature was 36 million degrees, this gives 10^{46} cm^{-3}. If one assumes typical upper chromospheric densities of about 10^{10} cm^{-3} and a height of 10^9 cm, the area of which need be bright at this temperature is exceedingly small; on the order of 3 millionths of the solar disc. Thus a very small chromospheric region which had either a higher temperature or an equivalent distribution of non-thermal electrons could account for the excess X-rays observed over the 10 to 20 keV range on March 15.

In addition to the "quiet" sun, we observed many X-ray increases of widely different characteristics. These have been extensively analyzed over the period from March 8 to March 23, when approximately 70 events occurred. The coverage during this interval was about 60%. In general, every flare is associated with the production of X-rays. The converse is not always true, at least for events reported in the monthly Solar-Geophysical Data of the Institutes for Environmental Research (ESSA).

The typical event has a fast onset and a slower recovery, with a duration of about 15 minutes. The burst frequency decreases rapidly with burst size. As indicated in Table I, during this 2-week period, approximately five bursts per day emitted a peak flux'of at least 1.2×10^{-6} ergs/cm^2 -sec. For bursts with peak intensity of greater 12×10^{-6} ergs/cm^2 -sec, the frequency was about 0.5 per day. This corresponds to 1000 counts/cm^2 -sec in the lowest channel. The instrument saturated at about 3000 counts/cm^2 -sec due to the width of the electronic enable gate.

A typical medium sized burst is shown in Figure 6. This burst was observed on the 16th of March and shows the correlation of microwave radio flux and the visible flare!**) Typically, we observe that the rise time of the event on the order of a few minutes while decay time is somewhat longer, on the order of 10 minutes. In all events thus far the higher energy X-rays show a faster decay time than the lower energy X-rays. Although this particular burst morphology is typical, many other forms have been observed, such as events that have very gradual rise or fall times. Excluding the very large events, the average rise time observed was

65 seconds, the average fall time was 340 seconds. Detailed correlations of these events with optical and radio observations, and with other observations on the OSO-III, have not yet been made.

One of the characteristics of these events is shown in the scatter diagram of Figure 7. Here is plotted the ratio of channel 3 to channel 2, which is a measure of the hardness of the X-ray spectrum, as a function of the peak intensity for each event. This shows clearly that the larger the X-ray event, the harder the spectrum. This rather unexpected result appears to be unambiguous at this time. On the basis of a thermal model this result suggests that the $n_e^2 V$ product for the radiating region tends to favor a value of approximately 10^{47} cm^{-3}.

It is interesting to compare the event shown in Figure 8, which occurred on March 20, with the burst shown in Figure 6. The peak flux of each corresponds to the 0.5 bursts per day occurrence frequency discussed above. Both show the characteristic fast rise and slow decay, and both show faster decay at higher energies in accordance with Figure 7. The March 20 burst had much greater duration, as did its related $H\alpha$ flare. However, the times of peak radio flux and $H\alpha$ emission showed no simple correlation with the times of peak X-ray emission. We conclude that even though the solar X-ray bursts obey certain well-defined laws (Figure 7), each burst is in a sense unique.

In addition to the quiet sun and to the many small bursts, we occasionally observe exceedingly large events, some of which cause saturation. The largest event of this period occurred on March 22 at approximately 0030 UT. This event has'been analyzed in some detail for monochromatic X-ray emis-

sions over the 13 to 1.3 Å range by Neupert.[7] Our data for this event are shown in Figure 9. The time scale here is much longer than that of the previously discussed events. The large flux of X-rays saturated the instrument electronics for more than an hour. Each gap in the data represents either a station readout of the OSO tape recorder or an interval during which the OSO satellite was in its night phase. The intensity of the X-rays in the 65 to 120 keV range was well above background for nearly an hour. Lower energy components remained above background for 3 or 4 hours and had not completely died away when another event occurred. Figure 9 also shows the approximate profile of 2700 megacycle radio emission as observed up to the time of radio sunset at the reporting station. It is not the intent here to go into a detailed analysis of these events, but merely to present data that is typical of hard solar X-ray observations on the OSO-III.

VI. Acknowledgements

The authors gratefully acknowledge the efforts of the many student and staff personnel in the X-ray and y-ray Astronomy Group at the University of California, San Diego, who have contributed to this project. The instrument was designed and constructed in a most expeditious manner by Mr. Don Hicks and Mr. Lou Reid of the Ball Brothers Research Corporation, Boulder, Colorado. The satellite was also designed, constructed and the payload integrated at the Ball Brothers Research Corporation. The OSO Program is supported by the National Aeronautics and Space Administration through the Goddard Space Flight Center. The OSO Project received its initial impetus from the late Dr. John C. Lindsay,

Mr. L. T. Hogarth is the Project Manager at Goddard Space Flight Center. The work at the University of California, San Diego is supported under NASA Contract NAS5-3177 through the Goddard Space Flight Center.

REFERENCES

1. Hicks, D. B., L. Reid, Jr. and L. E. Peterson, X-ray telescope for an orbiting solar observatory, 11th Nuclear Science Symposium, IEEE Trans. on Nuc. Sci., 12, 54-65, 1965.
2. Peterson, L. E., R. L. Jerde and A. S. Jacobson, Balloon X-ray Astronomy, AIAA J., 5, 1921, 1967.
3. Metzger, A. E., E. C. Anderson, M. A. Van Dilla, J. R. Arnold, Detection of an interstellar flux of gamma-rays, Nature, 204, 766-767, 1964.
4. Bleeker, J. A. M., J. J. Burger, A. Scheepmaker, N. B. Swanenburg and Y. Tanaka, Balloon observation of the isotropic component of celestial X-rays up to 90 keV, The Royal Dutch Academy of Sciences Preprint, February 1966.
5. Gould, Robert J., Origin of cosmic X-rays, Am. Jour. of Phys., 35, 376-393, 1967.
6. Arnoldy, R. L., S. R. Kane and J. R. Winckler, Energetic solar flare X-rays observed by satellite and their correlation with solar radio and energetic particle emission, Univ. of Minnesota TR CR-97, (submitted to Ap. J.), 1967.
7. Neupert, W. M., W. Gates, M. Swartz and R. Young, Observation of the solar flare X-ray emission line spectrum of iron from 1.3 to 20 Å, Ap. J. Ltrs., 149, 79-83, 1967.
8. Teske, R. G., Soft solar X-rays observed from OSO-III: Preliminary results, (Preprint, Aug. 25, 1967).
9. Chodil, G., R. C. Jopson, Hans Mark, F. D. Seward and C. D. Swift, X-ray spectra from Scorpius (SCO-XR-1) and the sun observed above the atmosphere, Phys. Rev. Ltrs., 15, 605, 1965.
10. Seward, F. D., and A. Toor, Search for 8-80 keV X-rays from the large Magellanic Cloud and other cosmic sources, UCRL-70300 preprint, 1967.
11. Institutes for Environmental Research, Solar-Geophysical Data, 272, April 1967.

TABLE I

Channel 2 - 7.7-12.5 Kev

Source	Rate (c/cm2-sec.)	Flux (ergs/cm^2-sec.)
Cosmic Sky Background	0.2	3×10^{-9}
"Quiet" Sun - March 15	3.0	50×10^{-9}
Bursts ~ 5/day	80	1.2×10^{-6}
Bursts ~ 0.6/day	1000	15×10^{-6}
Saturation	3000	50×10^{-6}

FIGURE CAPTIONS

Figure 1 The hard X-ray detector on the OSO-III. The active anti-coincidence shield provides collimation and excellent back-gound rejection. Events in the central detector are analyzed in a logarithmically spaced pulse-height analyzer over the 7.7 to 210 keV range.

Figure 2 The locus of wheel scans at various dates across the celestial sphere. On the scan of May 11th, the effect due to the finite detector aperture is also indicated. This scan initiates near the ecliptic plane, passes through the galactic center, near the strong source Scorpius XR-1 and into the northern skies.

Figure 3 Relative intensity across the scan path obtained during approximately 10 orbits on May 11th. The sun, the galactic center and Scorpius XR-1 are clearly visible above background.

Figure 4 The diffuse cosmic X-ray flux observed on the OSO-III. The flux, when no strong sources are known to be in the aperture, is corrected for the detector background, which has been obtained in a series of preliminary balloon and satellite investigations. The resultant flux agrees with previous measurements obtained on the Ranger-111.

Figure 5 The hard X-ray continuum of the nominally quiet sun obtained by various rocket observations and on the OSO-111 during this solar cycle. On March 15, the sun was generally active, although there were no visible flares or other events reported during the time this data was taken. During the period of May 11th only an upper limit was obtained because the flux was at a very low level.

FIGURE CAPTIONS (continued)

Figure 6. Solar X-ray event typical of those observed between March 8 to March 23, 1967. Some 10 events of this size occurred during this period, generally associated with solar flare or radio emission. The typical event shows a fast rise time and a slower decay time.

Figure 7 This shows the intensity of each event plotted as a function of the counting rates in the 12.5 - 22 keV channel divided by the 7.7 - 12.7 keV channel. This indicates that the more intense the event, the harder the apparent X-ray spectrum. The temperatures refer to a thermal bremsstrahlung source.

Figure 8 An X-ray event observed on March 20, 1967. This event, which was quite intense, is somewhat atypical because of the very slow decay time. The X-ray flux was in its decay phase at the time of flare H_α maximum. The fast rise was associated with the peak microwave emission.

Figure 9 The large event of March 22, 1967. The lower channels were completely saturated for many hours. Even at energies of 100 keV, a detectable intensity was emitted for nearly an hour. This shows clearly the softening of the spectrum with time.

Preliminary Results of the University of California X-Ray Experiment on the OSO-III*

Laurence E. Peterson, Hugh S. Hudson
and Daniel A. Schwartz
University of California, San Diego
La Jolla, California

I. Introduction

In this report we wish to describe the University of California X-ray experiment on the Third Orbiting Solar Observatory (OSO-III), indicate its present operational status and present a preliminary discussion of the results which have been obtained thus far. An OSO satellite consists of two parts: a telescope mount pointed at the sun and a rotating wheel member. The pointed section, which is maintained to within about 1 arc minute, contains instruments which generally cover the ultraviolet and soft X-ray range. The rotating wheel provides a stabilized platform for the pointed member, contains telemetry and servo systems and may be outfitted with additional experiments, generally of a somewhat different nature than those provided in the pointed section. The OSO's are launched into a nominally circular orbit of 33° inclination

*Based on presentations at the 13th International Astronomical Union Meeting, Prague, Czechoslovakiz, August 21-30, 1967, and at the OSO-III Review Conference, Goddard Space Flight Center, October 6, 1967.

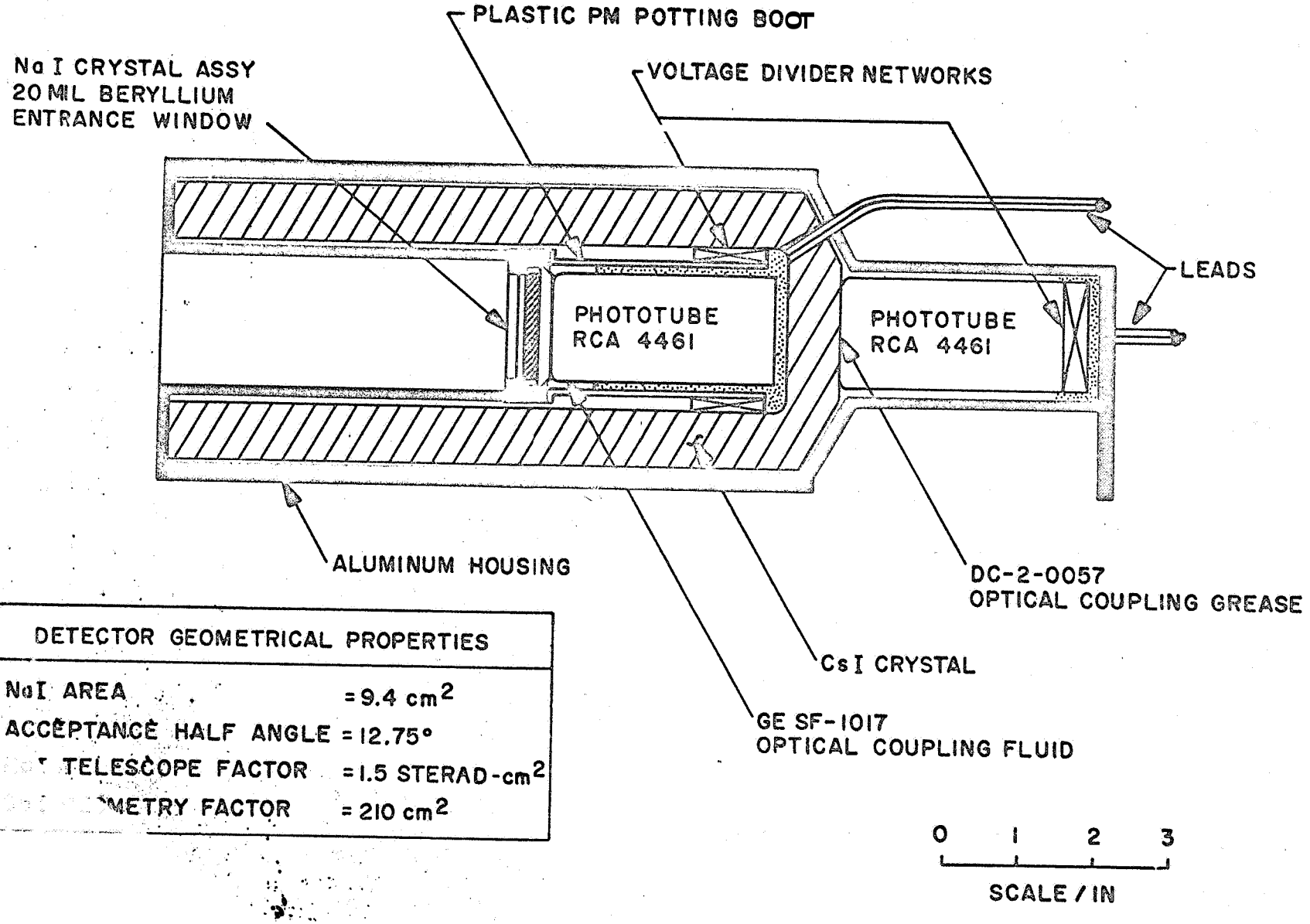

DETECTOR GEOMETRICAL PROPERTIES	
NaI AREA	$= 9.4\ cm^2$
ACCEPTANCE HALF ANGLE	$= 12.75°$
TELESCOPE FACTOR	$= 1.5\ STERAD\text{-}cm^2$
METRY FACTOR	$= 210\ cm^2$

Figure 1

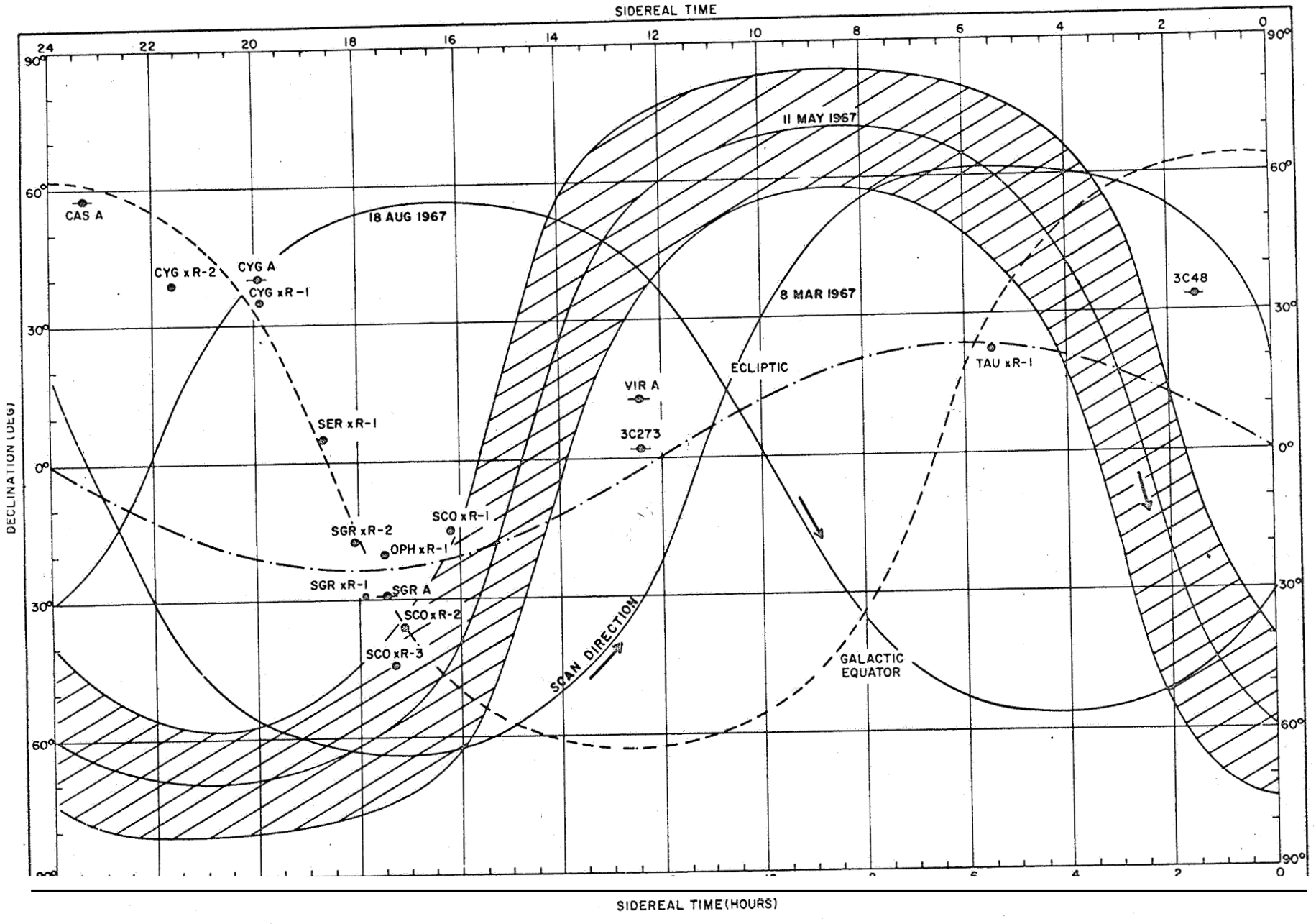
SIDEREAL TIME
24
22
20
18
16
14
12
10
8
6
4
2
0
90°
60°
30°
0°
DECLINATION (DEG)
CAS A
CYG x R-2
CYG A
CYG x R-1
SER x R-1
SGR x R-2
OPH x R-1
SCO x R-1
SGR x R-1
SGR A
SCO x R-2
SCO x R-3
18 AUG 1967
11 MAY 1967
8 MAR 1967
VIR A
3C273
ECLIPTIC
TAU x R-1
3C48
SPAN DIRECTION
GALACTIC EQUATOR
SIDEREAL TIME (HOURS)

Figure 2

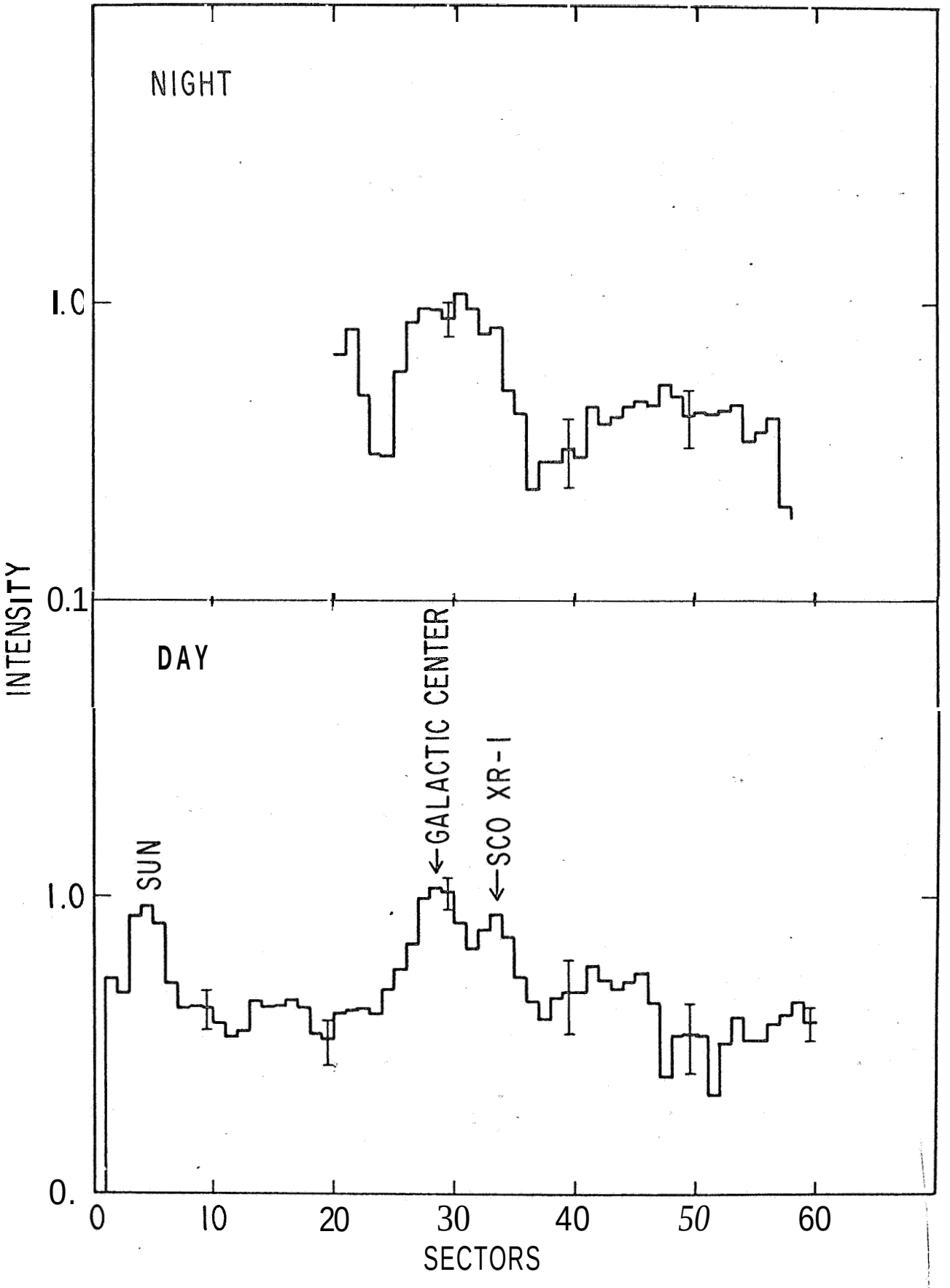
NIGHT
1.0
0.1
INTENSITY
DAY
GALACTIC CENTER
SCO XR-1
SUN
1.0
0.
0
10
20
30
40
50
60
SECTORS

Figure 3

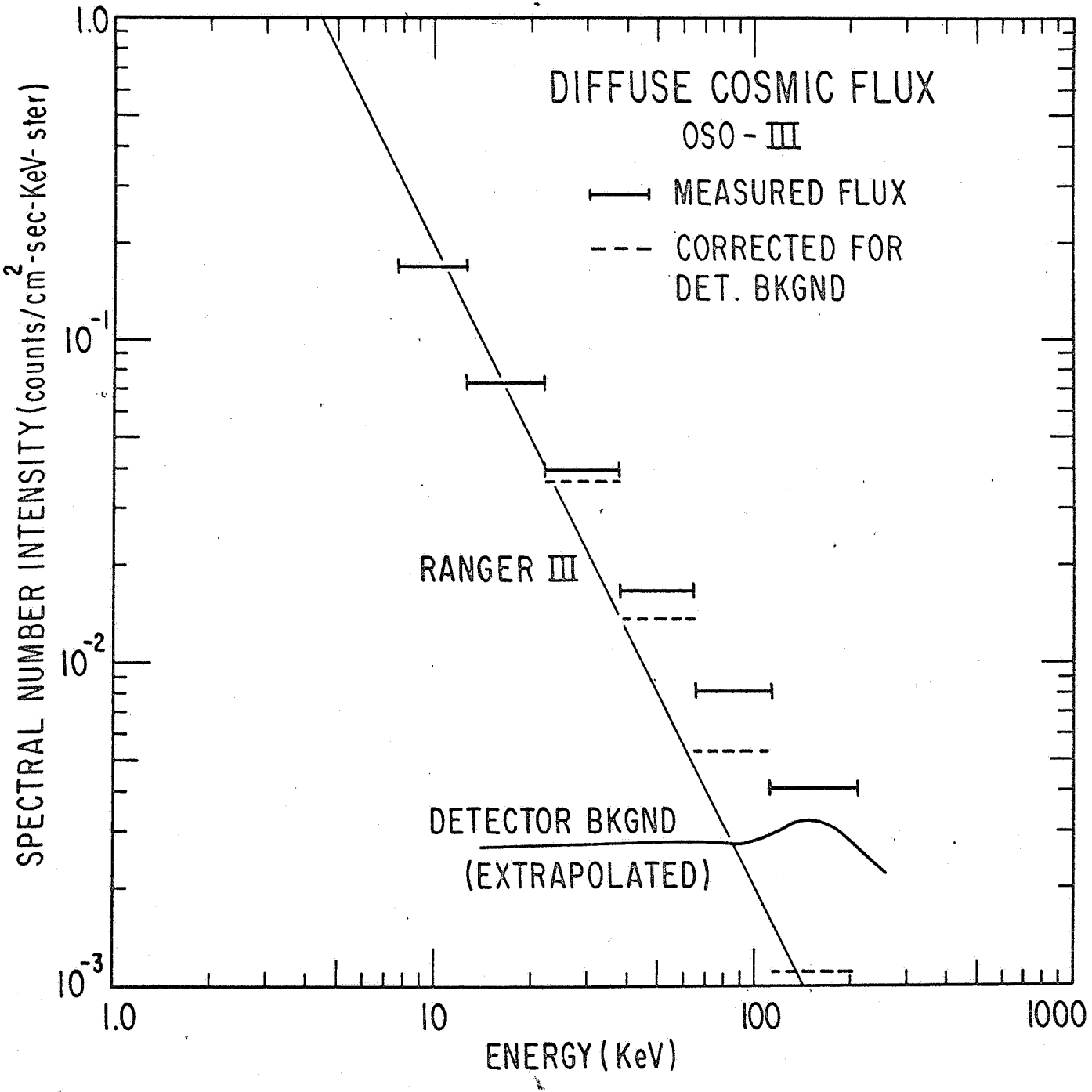
DIFFUSE COSMIC FLUX
OSO - III
MEASURED FLUX
CORRECTED FOR
DET. BKGND
RANGER III
DETECTOR BKGND
(EXTRAPOLATED)
SPECTRAL NUMBER INTENSITY (counts/cm²-sec-KeV-ster)
ENERGY (KeV)
1.0
10⁻¹
10⁻²
10⁻³
1.0
10
100
1000

Figure 4

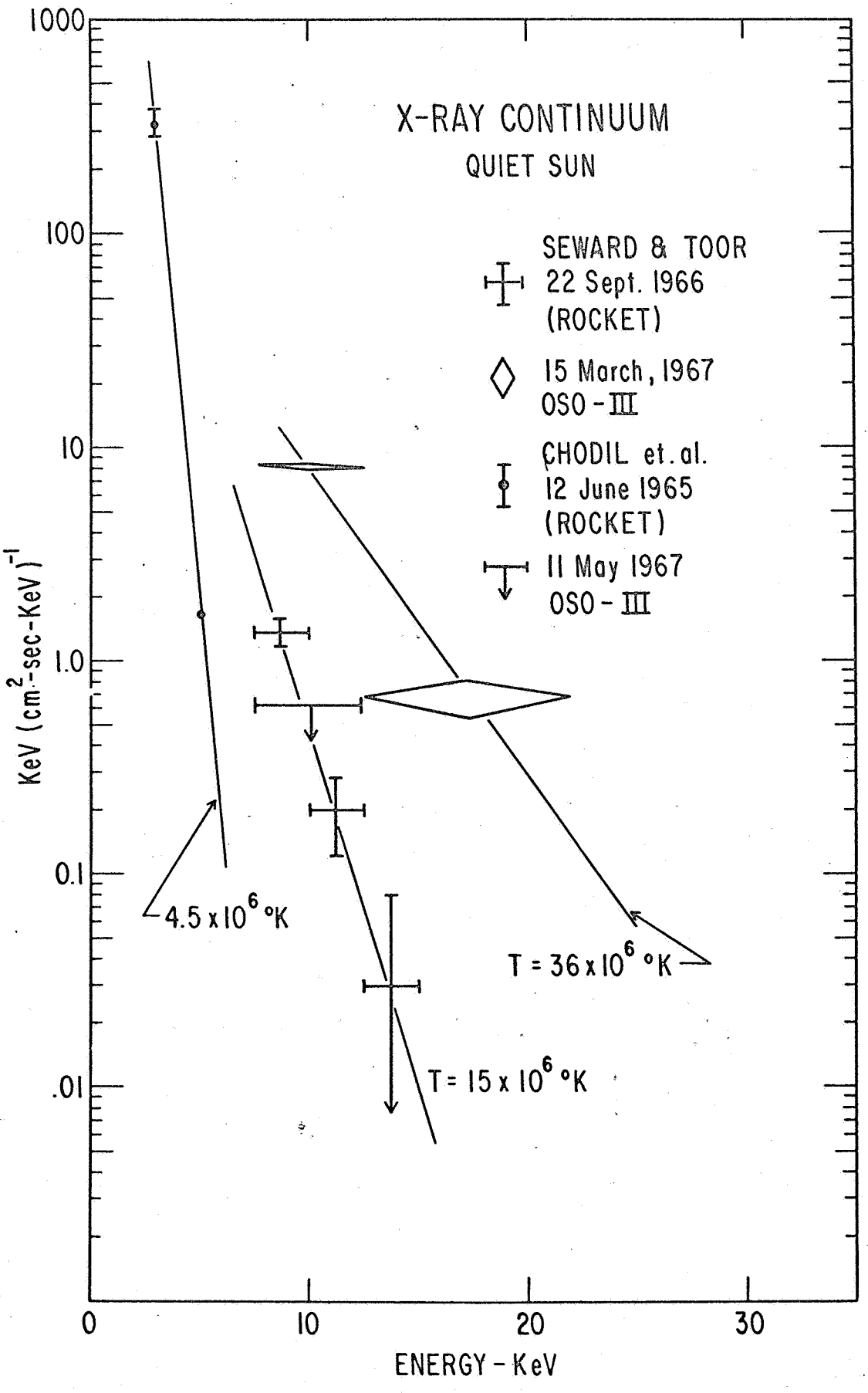
X-RAY CONTINUUM
QUIET SUN
SEWARD & TOOR
22 Sept. 1966
(ROCKET)
15 March, 1967
OSO - III
CHODIL et. al.
12 June 1965
(ROCKET)
11 May 1967
OSO - III
4.5 x 10^6 °K
T = 36 x 10^6 °K
T = 15 x 10^6 °K
KeV (cm.^2-sec-KeV)^-1
ENERGY - KeV
1000
100
10
1.0
0.1
.01
0
10
20
30

Figure 5

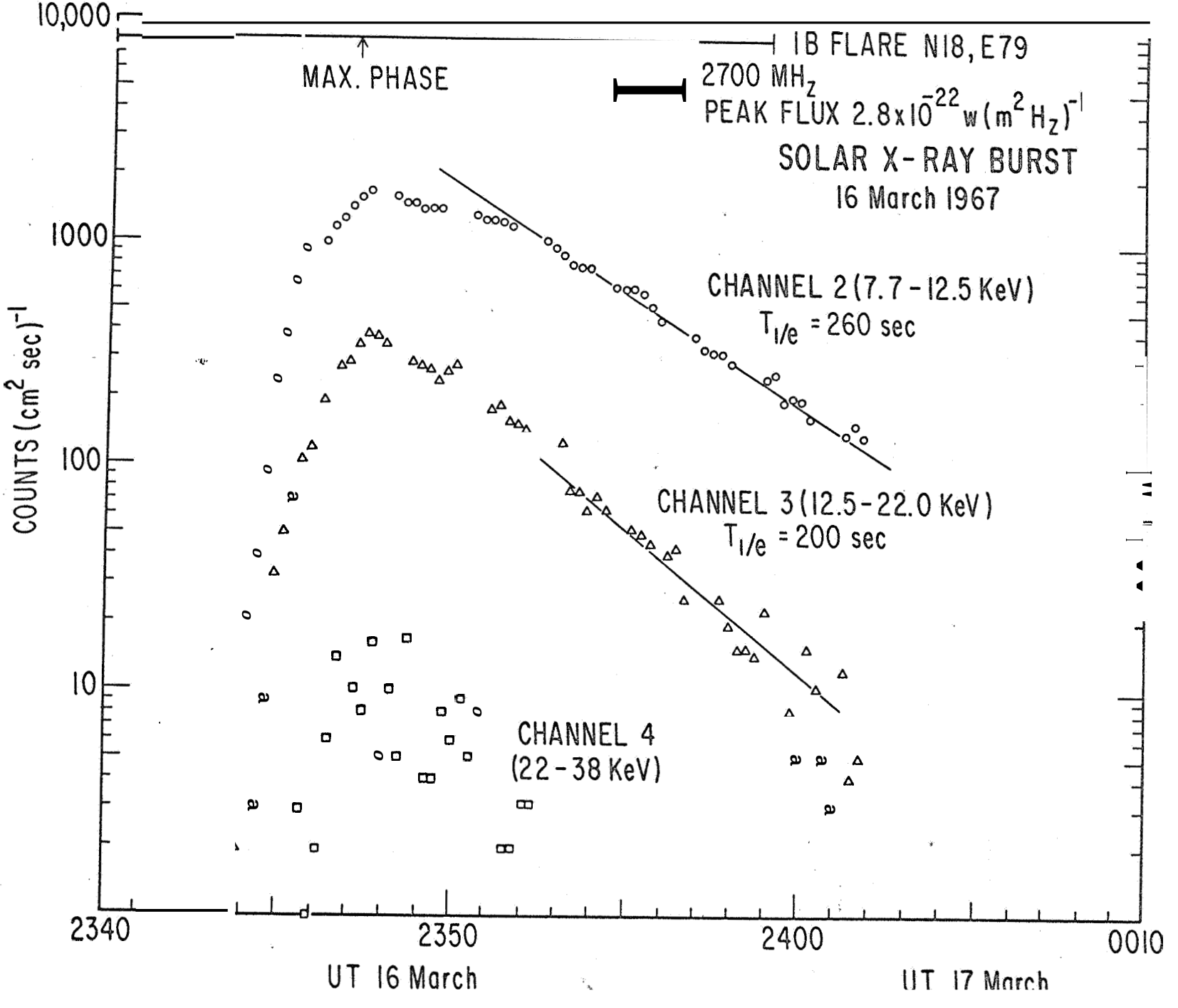
10,000
1000
100
10
COUNTS (cm² sec)⁻¹
MAX. PHASE
1B FLARE N18, E79
2700 MHz
PEAK FLUX 2.8x10⁻²² w(m² Hz)⁻¹
SOLAR X-RAY BURST
16 March 1967
CHANNEL 2 (7.7 - 12.5 KeV)
T1/e = 260 sec
CHANNEL 3 (12.5 - 22.0 KeV)
T1/e = 200 sec
CHANNEL 4
(22 - 38 KeV)
2340
2350
2400
0010
UT 16 March
UT 17 March

Figure 6

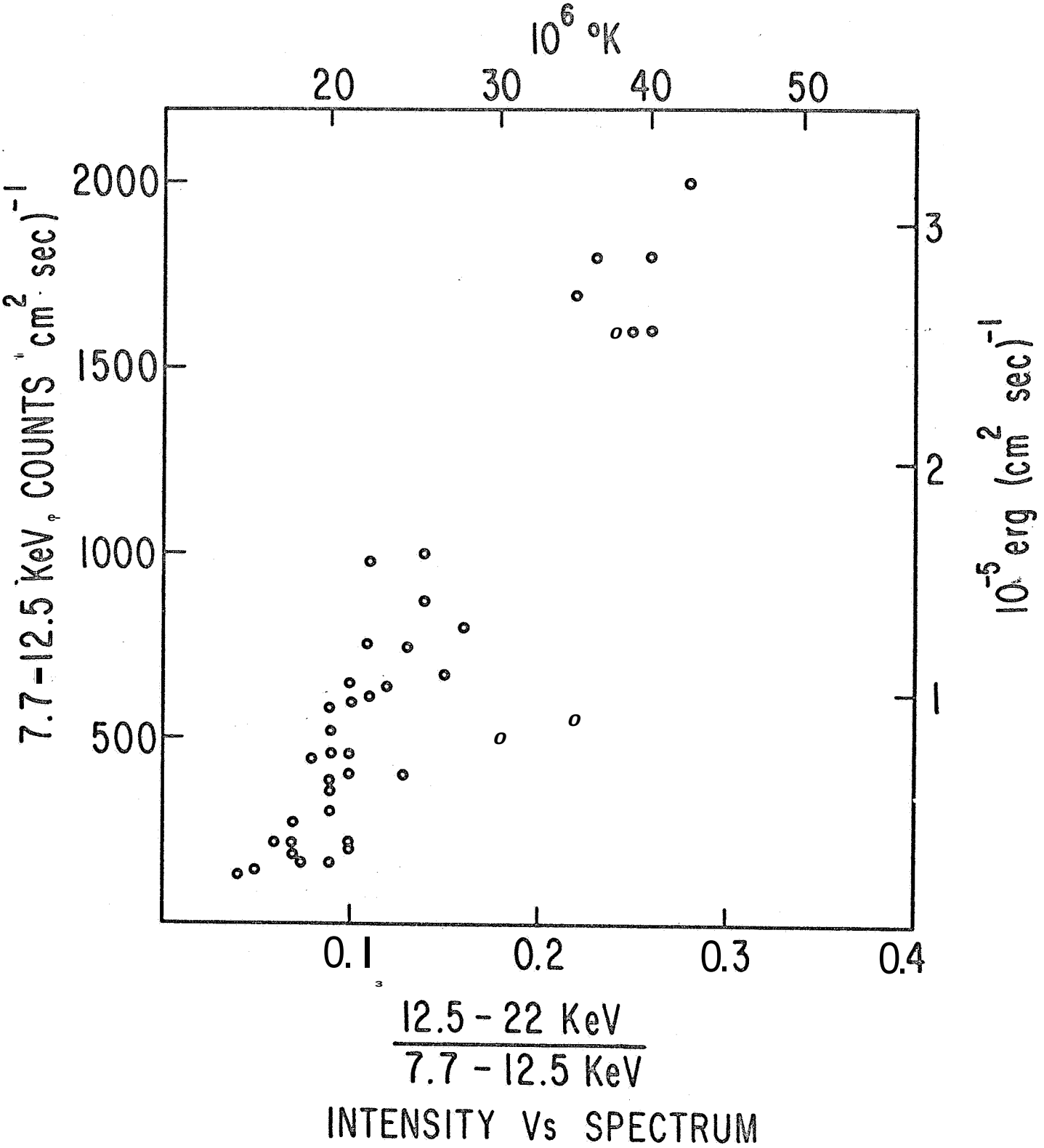
10^6 °K
20
30
40
50
2000
1500
1000
500
7.7 - 12.5 keV, COUNTS cm^2 $sec)^{-1}$
3
2
1
10^{-5} erg $(cm^2$ $sec)^{-1}$
0.1
0.2
0.3
0.4
12.5 - 22 KeV / 7.7 - 12.5 KeV
INTENSITY Vs SPECTRUM

Figure 7

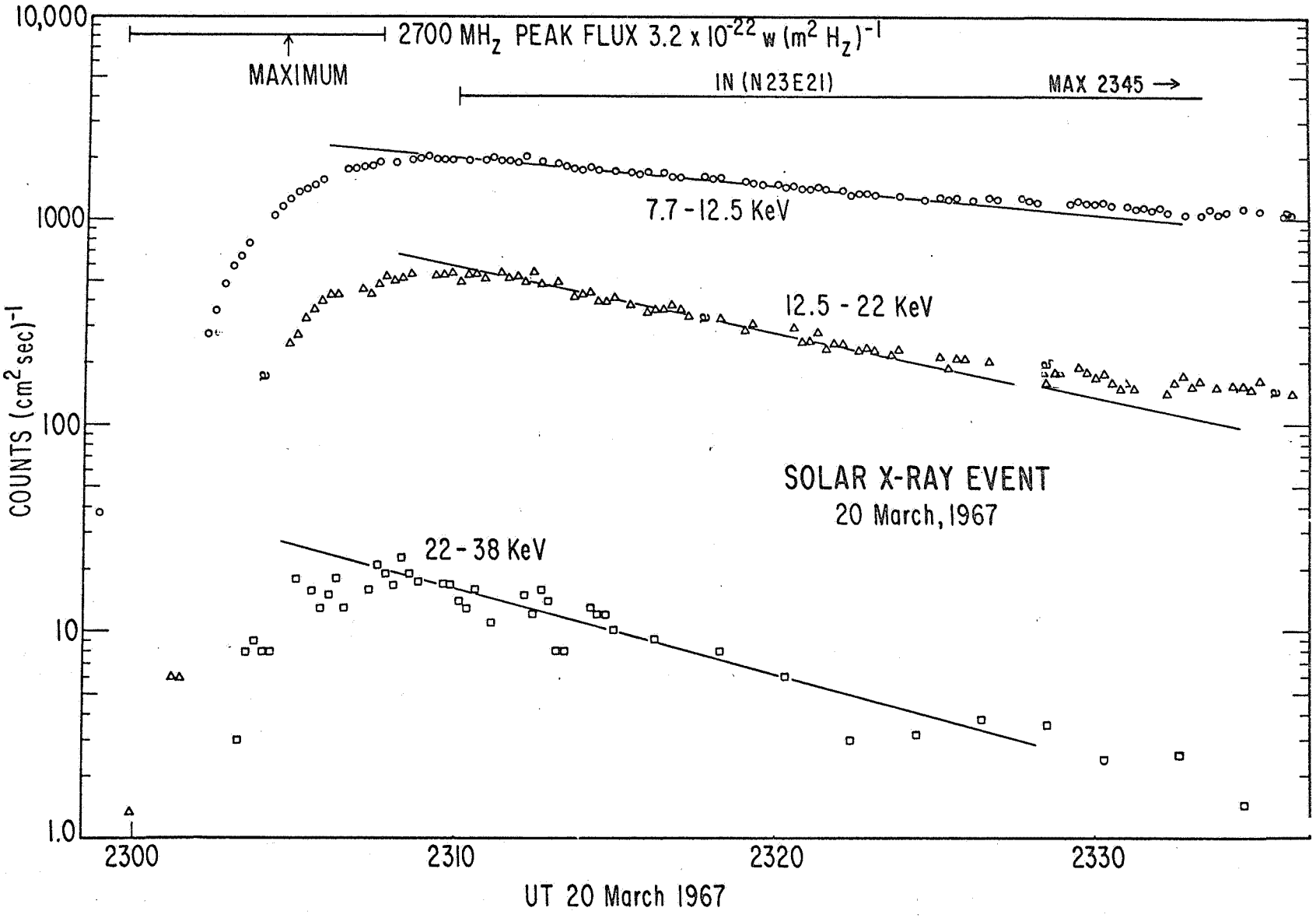
10,000
1000
100
10
1.0
COUNTS (cm² sec)⁻¹
2700 MHz PEAK FLUX 3.2 x 10⁻²² w (m² Hz)⁻¹
MAXIMUM
IN (N23E21)
MAX 2345 →
7.7 - 12.5 KeV
12.5 - 22 KeV
22 - 38 KeV
SOLAR X-RAY EVENT
20 March, 1967
2300
2310
2320
2330
UT 20 March 1967

Figure 8

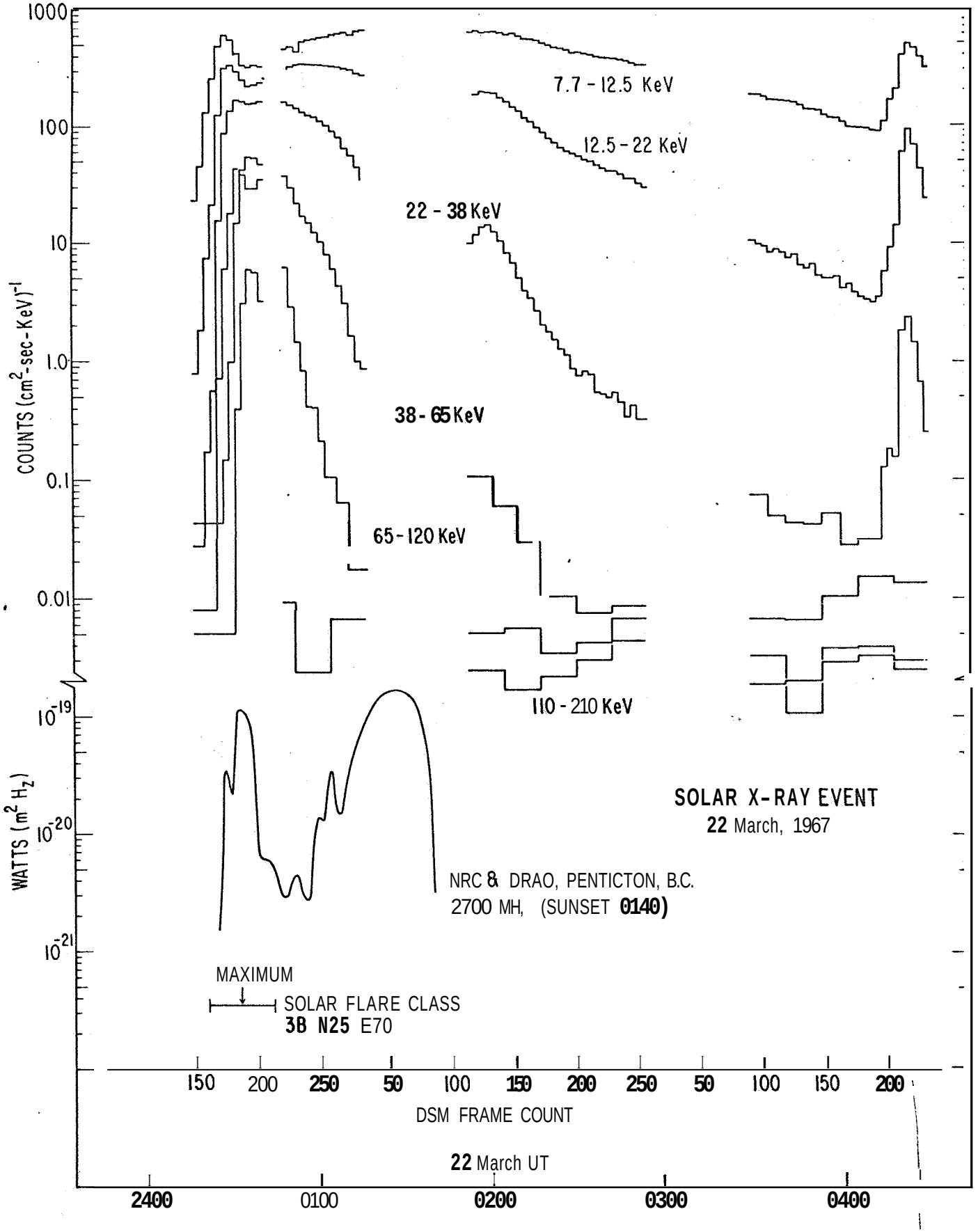
7.7 - 12.5 KeV
12.5 - 22 KeV
22 - 38 KeV
38 - 65 KeV
65 - 120 KeV
110 - 210 KeV
COUNTS (cm²-sec-KeV)⁻¹
WATTS (m² Hz)
SOLAR X-RAY EVENT
22 March, 1967
NRC & DRAO, PENTICTON, B.C.
2700 MH, (SUNSET 0140)
MAXIMUM
SOLAR FLARE CLASS
3B N25 E70
DSM FRAME COUNT
22 March UT
2400
0100
0200
0300
0400

Figure 9